
TREE TRAINING: ACCELERATING AGENTIC LLMs TRAINING VIA SHARED PREFIX REUSE

Shaojie Wang^{*†1} Jinghui Wang^{*†1} Yinghan Cui^{*1} Xuxing Chen^{*1} Chao Wang^{*1} Liang Huang¹
 Xiaojiang Zhang¹ Junyi Peng¹ Li Wan¹ Haotian Zhang¹ Bin Chen¹

ABSTRACT

Agentic large language model (LLM) training often involves multi-turn interaction trajectories that branch into multiple execution paths due to concurrent tool use, think-mode, sub-agent, context management and other runtime designs. As a result, the token produced by a single task naturally forms a tree-structured token trajectory with shared prefixes, rather than a linear sequence. Existing training pipelines linearize such trajectories and treat each branch independently, leading to substantial redundant computation in both forward and backward passes. To eliminate such redundancy, we introduce Tree Training, an efficient training framework for tree-structured trajectories. Its core component, Gradient Restoration, enables correct gradient aggregation across shared prefixes with negligible overhead, allowing each prefix to be computed exactly once while remaining mathematically equivalent to independent training on all branches. To support large trajectory trees in practice, we redesign the training engine to natively ingest tree-structured data and propose Tree Packing, a memory-efficient partitioning strategy that preserves high prefix reuse. Experiments conducted on dense and MOE models of real-world agentic trajectories show 6.2× training speedup for both supervised fine-tuning and the model update phase in reinforcement learning.

1 INTRODUCTION

Training Large Language Models (LLMs) in agentic scenarios involves multi-turn interactions with environments, where a single task frequently branches into multiple parallel paths. This branching is driven by tree-structured workflow designs (e.g., tree structured planning (Yao et al., 2023; Zhang et al., 2024) and sub-agents (Team et al., 2026)), concurrent tool invocations (Kim et al., 2024; Abdelaziz et al., 2024), context management (Xu et al., 2025; Packer et al., 2024; Zhong et al., 2023), as well as runtime behaviors such as think-mode (discarding/replacing intermediate reasoning tokens between turns, e.g. Figure 1), and retokenization drift (Luo et al., 2025). These mechanisms imply that the context fed into turn $t+1$ is often *not* exactly the concatenation of the tokens produced in previous turns (from turn 1 to turn t); therefore, after finishing a task, the collected tokens cannot always be organized as a single list/tensor, but instead form a tree-structured token trajectory with shared prefixes across branches. As a result, training must process multiple sequences with substantial shared prefixes, leading to significant redundant forward/backward computation.

^{*}Equal contribution ¹Kwai Inc. Correspondence to: Shaojie Wang <wangshaojie05@kuaishou.com>, Jinghui Wang <wangjinghui05@kuaishou.com>.

The decoder-only LLM’s generation is autoregressive and uses a causal attention mask. When we consider the inference scenario alone, prefix caching (Kwon et al., 2023; Pope et al., 2022) can eliminate redundant prefix computation: the causal mask prevents suffix tokens from influencing prefix tokens, so identical prefixes produce identical key/value states, which can be reused to avoid recomputing the prefix in the forward pass. In training, the backward pass “transposes” the causal masking pattern: to compute the gradient of a prefix token, one must aggregate gradient contributions and intermediate activations from *all* suffix tokens under that prefix. Therefore, to avoid repeatedly recomputing prefix tokens, caching approaches would have to store suffix information for all branches, which drastically inflates GPU memory usage and exceed practical training budgets, making such approaches infeasible in practice.

To address the above challenges, unlike caching-based approaches, we provide a strict mathematical derivation and develop an extremely low-overhead method, **Gradient Restoration**, to remove redundant prefix computation in the backward pass. Concretely, we apply a per-token compensation term so that each shared prefix is computed once while the resulting gradients are mathematically equivalent to training on all branches independently.

With this guarantee of efficient and correct prefix reuse, we further modify the training engine to ingest tree-structured

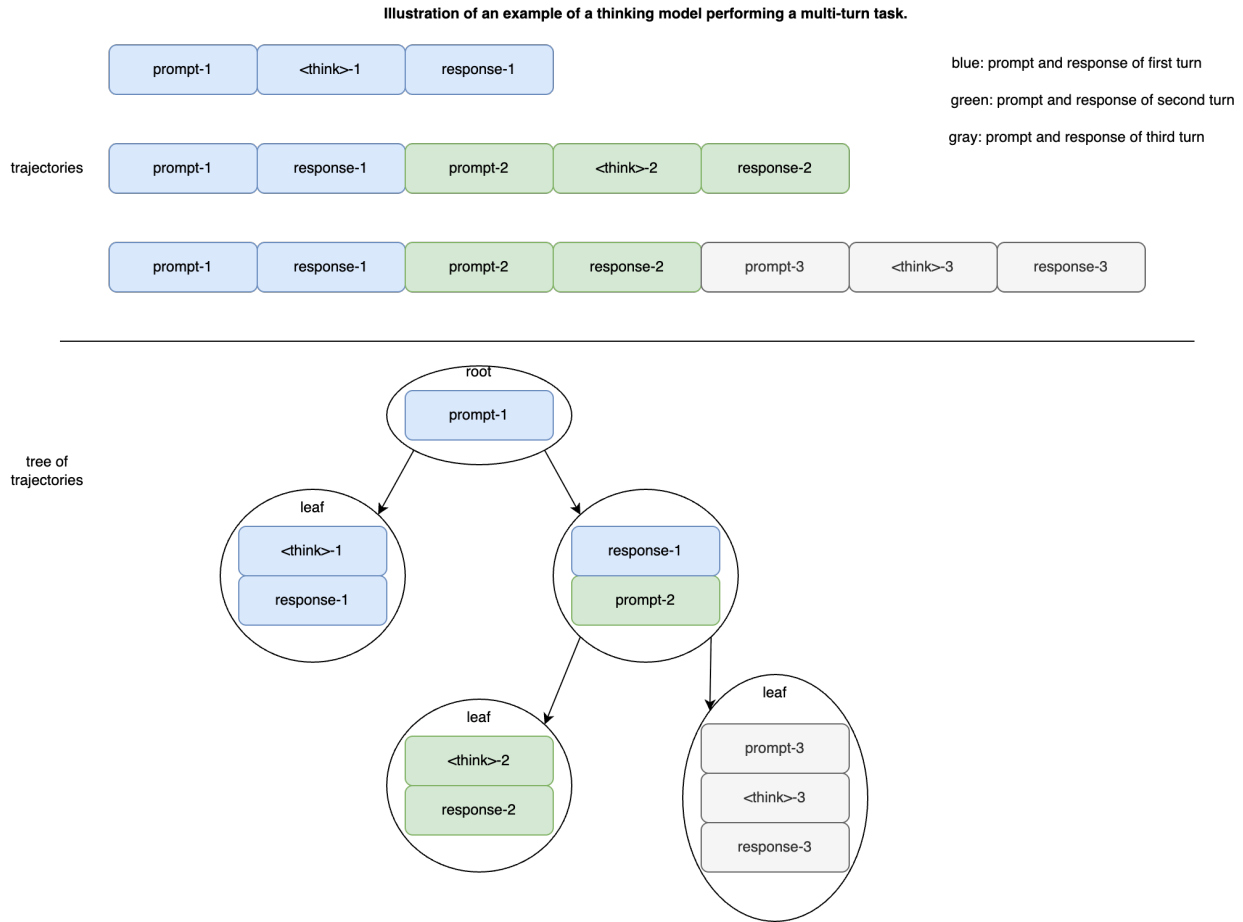


Figure 1. Illustration of shared prefixes. Illustration of an example of a thinking model performing a multi-turn task: three sequences correspond to the model inputs and responses in the 1st, 2nd, and 3rd turns, respectively. In each new turn, the thinking process from the previous turn is discarded. This results in a situation where the concatenation of the previous turn’s input and output is not equivalent to the context fed into the current turn. As a result, upon completion of this multi-turn interactive task, it is impossible to represent all generated tokens for the task using a single tensor. Consequently, training with multiple sequences that share large overlapping prefixes leads to significant redundant computation.

trajectory data (where existing training frameworks (Paszke et al., 2019; Abadi et al., 2016) typically only support list-like tensors). We also identify and address a practical issue for tree-structured training: a single trajectory tree can be too large to fit entirely within GPU memory, so we must partition a large tree into multiple subtrees and process them in multiple steps. The partitioning must ensure that each subtree fits in memory while preserving a high prefix-reuse ratio to achieve near-optimal compute efficiency. We implement **Tree Packing** with a heuristic DFS partitioning strategy, which is highly effective in practice and yields performance that closely approaches the theoretical limit.

Together, Gradient Restoration, Tree Packing, and a tree-aware training-engine redesign form **Tree Training**: an efficient framework for training LLMs on arbitrary tree-structured trajectories for both SFT and RL (reinforcement

learning), achieving up to **6.2×** end-to-end training speedup in our experiments.

In summary, our contributions are threefold:

- (1) We identify a pervasive yet overlooked property of agentic LLM training: trajectories naturally form overlapping tree-structured prefixes, creating substantial opportunities for computation reuse.
- (2) We introduce **Tree Training**, a paradigm that executes each shared prefix once while correctly aggregating activations and gradients across descendant branches through Gradient Restoration, Tree Packing, and the redesign of the training engine.
- (3) We demonstrate consistent gains across dense and MOE (DeepSeek-AI et al., 2024) models on diverse datasets, achieving average 6.2× end-to-end speedup—and in agentic

RL scenarios—without compromising training fidelity or final model quality.

2 RELATED WORK

Prefix caching is widely used to speed up autoregressive decoding by reusing identical prefixes in the forward pass (Kwon et al., 2023; Pope et al., 2022; Liu et al., 2024; Cheng et al., 2024; Yao et al., 2025; Cheng et al., 2025; Qin et al., 2025). For training objectives where the shared part is purely a prompt, batching strategies such as prefix grouping can also reuse the prompt prefix computation without affecting gradients (Liu et al., 2025; Wang & Hegde, 2024). In addition, Goru et al. (Goru et al., 2025) propose a custom-mask approach to deduplicate repeated reasoning tokens within a single linear conversation. However, it does not address prefix reuse across multiple trajectories, and its prefixes never aggregate loss from multiple branches. As a result, it is a special case of the agentic scenario where the backward pass remains standard.

Prior works have also recognized that agentic/RL generation often forms tree-structured rollouts, and exploit shared prefixes primarily to improve *rollout* efficiency, e.g., tree-search style rollouts and prefix reuse (Hou et al., 2025; Li et al., 2025; Ji et al., 2025). However, the subsequent training stage is commonly executed on linearized samples: current training pipelines (Luo et al., 2025; Zhang et al., 2025; Zhou et al., 2025) typically decompose a trajectory tree into separate linear segments and treat each segment independently, causing shared prefixes to be repeatedly recomputed in both forward and backward passes.

Sequence packing (Krell et al., 2021) refers to concatenating multiple short sequences into a fixed-length training example to improve training efficiency. Our proposed tree packing method generalizes this idea: it not only concatenates sequences, but also introduces a strategy for efficiently segmenting overly long training data structured as a prefix tree (noting that a sequence is a special case of a prefix tree).

Overall, unlike our work, these methods primarily target inference-time caching, prompt-only reuse, or single-conversation masking, and do not address the general case where a shared prefix must aggregate gradient contributions from multiple continuations.

3 TREE TRAINING

3.1 Overview

The standard approach for reusing computations of a shared prefix across two sequences is to employ prefix-caching. Although it is effective during inference and the forward pass of training, it can not be applied on the backward pass. Figure 2 showed this asymmetry in forward and backward

passes of the attention operator.

Forward Passes The forward pass of attention is expressed as:

$$\begin{aligned} S &= Q \times K^T \\ P &= \text{softmax}(S) \\ O &= P \times V \end{aligned} \tag{1}$$

Due to the causal masking mechanism, the attention matrix P is a Lower Triangular Matrix. The output O_i for the i -th token depends solely on the token itself and its preceding tokens ($j \leq i$). Consequently, identical prefixes across different sequences share identical P and V matrices for the prefix positions, guaranteeing that their outputs are identical (i.e., $O_1 \equiv O'_1$ in Figure 2). This enables caching feasible and effective.

Backward Passes The backward pass of V is expressed as:

$$dV = P^T \times dO \tag{2}$$

The transposition transforms the matrix P into P^T , which is an Upper Triangular Matrix and is anti-causal. This implies that the gradient dV_i for the i -th token aggregates gradients from the token itself and all subsequent tokens ($j \geq i$). Even if two sequences share an identical prefix, their differing suffixes introduce distinct dO_{suffix} , which propagate backward to the prefix. As a result, the gradients for the identical prefix positions (dV_{prefix}) will diverge (i.e., dV_1 and dV'_1 in Figure 2).

While the forward pass is causal (prefix affects suffix), the backward pass is anti-causal (suffix affects prefix). Caching intermediate states for the backward pass is therefore not feasible across different suffixes, as the gradient computation for the prefix is inextricably coupled with the specific content of the entire suffix, making such caching memory-inefficient. To address these, we propose gradient restoration method in Section 3.2. Although our solution eliminates redundant computation, it needs a new data packing algorithm for large trees, which will be introduced in Section 3.3.

3.2 Gradient Restoration

During the backward pass, the gradients of the prefix tokens are no longer identical across different sequences. The primary challenge, therefore, lies in determining how to eliminate gradient discrepancies such that the shared prefix can be computed only once across packed sequences, while preserving computational correctness.

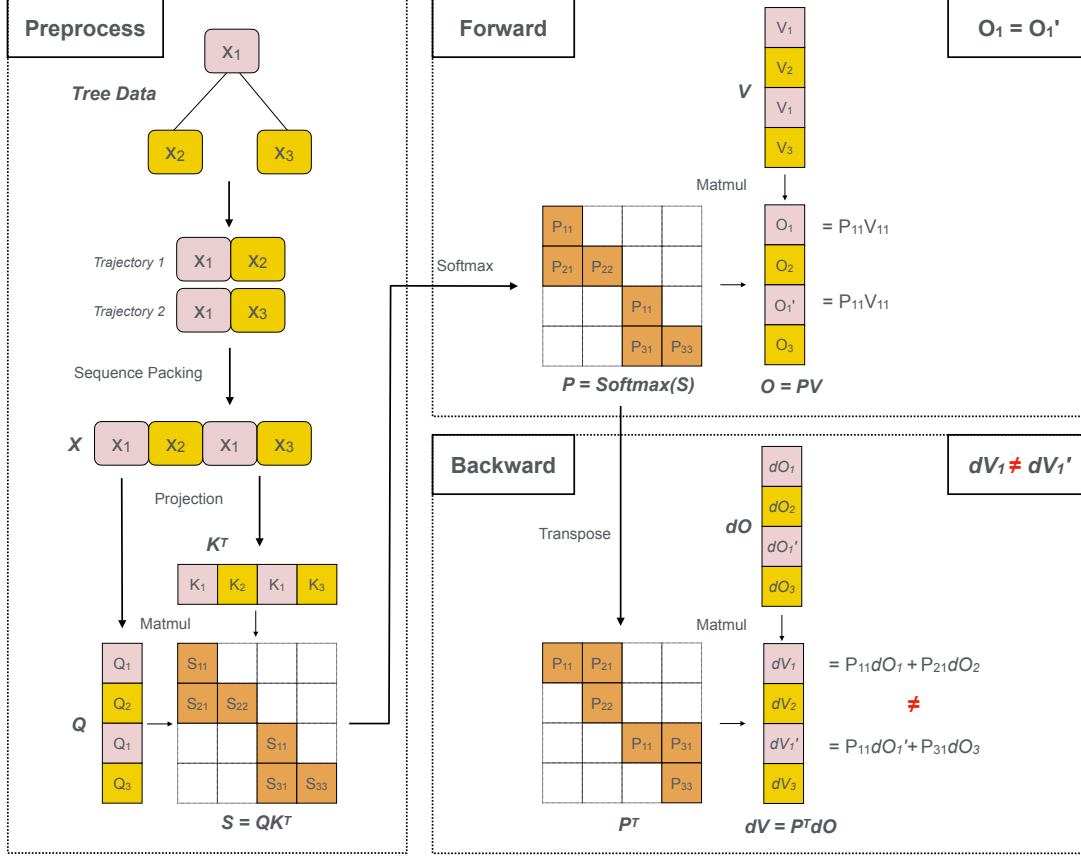


Figure 2. Schematic of the data preprocess, forward pass, and backward pass in a tree-structured dataset. Pink blocks represent the prefix, yellow blocks correspond to two suffixes. The $(Q_1, K_1, V_1, O_1, dO_1, dV_1)$ correspond to the query, key, value, output, gradient of output and gradient of value matrices of the shared prefix between the two sequences. S_{mn} denotes the result of the matmul between Q_m and K_n , P_{mn} denotes the result obtained by applying the softmax function to S_{mn} . In the **forward pass**, the outputs O_1 and O_1' are identical, thus making caching feasible. In the **backward pass**, the intermediate dV_1 and dV_1' are not identical, thus making caching unfeasible.

We next contrast the baseline and our method in terms of backpropagation, and derive a gradient restoration algorithm that compensates for the gradient loss introduced by omitting redundant computations on shared prefixes.

3.2.1 baseline method

The baseline aligns with the current standard practice for training on branched trajectories, as most existing training frameworks only support taking batches of list-like tensors as training inputs. Specifically, for each leaf node in a trajectory tree, we construct a sequence by tracing back all tokens along the path from the leaf to the root; each leaf node thus corresponds to one sequence. These sequences are then processed through forward and backward passes individually, and the gradients accumulated across them are used to compute the overall gradient corresponding to the trajectory tree. However, this approach repeatedly recomputes shared prefixes across branches, leading to excessive redundant

computation and thus an impractically long training time.

3.2.2 Parameter Updates with Gradients

We use a recursive definition over the trajectory tree. Here i is the index of a tree node; $\text{token}(i)$ denotes the token sequence represented by node i ; $\text{child}(j, i)$ denotes the index of the j -th child of node i (and returns empty if node i is a leaf node); and $X(i)$ denotes the list obtained by serializing the subtree rooted at node i .

The baseline serializes the subtree by pairing the prefix tokens $\text{token}(i)$ with each child subtree, and concatenating these prefix-child pairs:

$$X_{\text{base}}(i) = \text{Concat}[\text{token}(i), X_{\text{base}}(\text{child}(0, i)), \text{token}(i), X_{\text{base}}(\text{child}(1, i)), \dots, \text{token}(i), X_{\text{base}}(\text{child}(m, i))] \quad (3)$$



Figure 3. **A Comparative Illustration of Backward V-Gradient Computation and the Baseline.** Pink blocks represent the (Q, K, dO, dV) for the prefix parts, while yellow blocks correspond to those of the suffix parts. The orange blocks signify that their corresponding $(S$ or $P)$ values are active in the attention computation, whereas the white blocks indicate that their $(S$ or $P)$ values are masked out, the green blocks represent the $(S$ or $P)$ computations that can be omitted in our method.

Our method serializes the subtree by concatenating token(i) only once and reusing it across all children:

$$X_{ours}(i) = \text{Concat}[\text{token}(i), X_{ours}(\text{child}(0, i)), X_{ours}(\text{child}(1, i)), \dots, X_{ours}(\text{child}(m, i))] \quad (4)$$

It suffices to show that performing backward on $X_{ours}(i)$ yields gradients equivalent to performing backward on $X_{base}(i)$ for the 2-level subtree consisting of node i and its children; by recursion, this guarantees equivalence over the entire tree.

Therefore, we can focus on a simplified 2-level case. To avoid an abuse of notation, we let X denote the serialized list of a root node with n children. For a linear transformation: $Y = X \times \text{weight}$. The gradient $d \text{weight} = X^T \times dY$.

In the baseline serialization, we can view the process as first forming n prefix-suffix pairs, each consisting of the shared prefix P and one suffix S_i , and then concatenating these pairs together. Concretely, the matrix X serialized by the

baseline method is:

$$x_i = [P; S_i], \forall i \in [1, n] \quad (5)$$

$$X_{base} = [x_1; x_2; \dots; x_n]$$

In contrast, the matrix X obtained by our serialization method is:

$$X_{ours} = [P; S_1; S_2; \dots; S_n] \quad (6)$$

where P denotes prefix token, S denotes suffix token.

The computation of $d \text{weight} = X^T * dY$ can be interpreted as each column of X^T multiplied by each row of dY , which yields the contribution of token_i to the entire weight gradient, denoted as $d \text{weight}_i$. The total $d \text{weight}$ is equal to the sum of the $d \text{weight}_i$ for each individual token. Hence, if we can ensure that:

$$P^T \times dY_P^{ours} = P^T \times \left(\sum_{i=1}^n dY_{p_i}^{base} \right) \quad (7)$$

We can guarantee that the contribution of the prefix P to $d \text{weight}$ in our method will be equivalent to its contribution

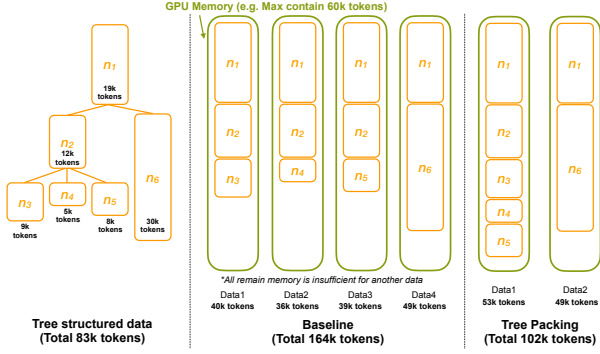


Figure 4. Illustration of Tree Packing under memory constraints. Ideally, tree packing merges all trajectories into a single sequence to maximize prefix sharing. However, when the total tree size (e.g., 83k tokens) exceeds the GPU memory limit (e.g., 60k tokens), our method partitions the tree into minimal sub-sequences. Compared to the baseline flattening approach (164k tokens), our method (102k tokens) significantly reduces redundancy.

in the baseline method. Equation 7 serves as the foundation for our gradient correction.

3.2.3 Algorithm and Analysis

In order to guarantee the equivalence of our Gradient Restoration method and the baseline method with respect to gradient updates, the two equations below must be identically satisfied for every trainable linear parameter.

$$\begin{aligned}
 P^T \times dY_P^{ours} &= P^T \times \left(\sum_{i=1}^n dY_{p_i}^{base} \right) \\
 \sum_{i=1}^n S_i^T \times dY_{S_i}^{ours} &= \sum_{i=1}^n S_i^T \times dY_{S_i}^{base}, \forall i \in [1, n]
 \end{aligned} \tag{8}$$

Given that the values of P and S are determined exclusively by the dataset, which is identical for both serialization methods, the requirement reduces to ensuring that:

$$\begin{aligned}
 dY_P^{ours} &= dY_{p_1}^{base} + dY_{p_2}^{base} + \dots + dY_{p_n}^{base} \\
 dY_{S_i}^{ours} &= dY_{S_i}^{base}, \forall i \in [1, n]
 \end{aligned} \tag{9}$$

The remainder of this chapter will focus on explaining how to achieve identical satisfaction of the two aforementioned equations in the Transformer model through a straightforward correction.

Linear Operation The linear operation is ubiquitous in the Transformer architecture. Assuming the following linear model:

$$Y = X \times weight \tag{10}$$

The gradient for the input, dX , used during backpropagation is calculated as follows:

$$dX = dY \times weight^T \tag{11}$$

The computation of $dX = dY \times weight^T$ can be viewed as each row of dY being multiplied by the entire matrix $weight^T$ to yield the corresponding row of dX . This shows that a *linear operation* is pointwise: each dX_i is obtained by multiplying dY_i by $weight^T$, without depending on the gradients of preceding or subsequent tokens. Therefore, during backpropagation, if Equation 9 holds, then:

$$\begin{aligned}
 dX_P^{ours} &= dX_{p_1}^{base} + dX_{p_2}^{base} + \dots + dX_{p_n}^{base} \\
 dX_{S_i}^{ours} &= dX_{S_i}^{base}, \forall i \in [1, n]
 \end{aligned} \tag{12}$$

Equations 9 and 12 reveal that the gradient correction is transitive across linear operations. In the overall training pipeline, we only need to insert a gradient scaling step before the backward propagation. This operation restores the correct influence of each sequence’s prefix on the model update, ensuring training consistency. At the same time, for linear-type computations, we can avoid redundant computation on shared prefixes altogether.

Attention Operation Assume $Q, K, V \in \mathbb{R}^{S \times d}$ are the inputs to the Attention Operation, where S denotes the sequence length and d is the head dimension. The forward pass and backward pass can be expressed as Equation 1 and Equation 2.

For the sake of clarity, this section will exemplify our gradient correction method for the attention operation using the computation of dV , which is illustrated in Figure 3.

Since the training dataset and weights (such as W_q and W_k) are consistent between the two packing methods, the S_{ij} and P_{ij} at corresponding positions are equal.

According to the matrix computation depicted in Figure 3, if the following condition holds:

$$\begin{aligned}
 dO_P^{ours} &= dO_{p_1}^{base} + dO_{p_2}^{base} + \dots + dO_{p_n}^{base} \\
 dO_{S_i}^{ours} &= dO_{S_i}^{base}, \forall i \in [1, n]
 \end{aligned} \tag{13}$$

then:

$$\begin{aligned}
 dV_P^{ours} &= dV_{p_1}^{base} + dV_{p_2}^{base} + \dots + dV_{p_n}^{base} \\
 dV_{S_i}^{ours} &= dV_{S_i}^{base}, \forall i \in [1, n]
 \end{aligned} \tag{14}$$

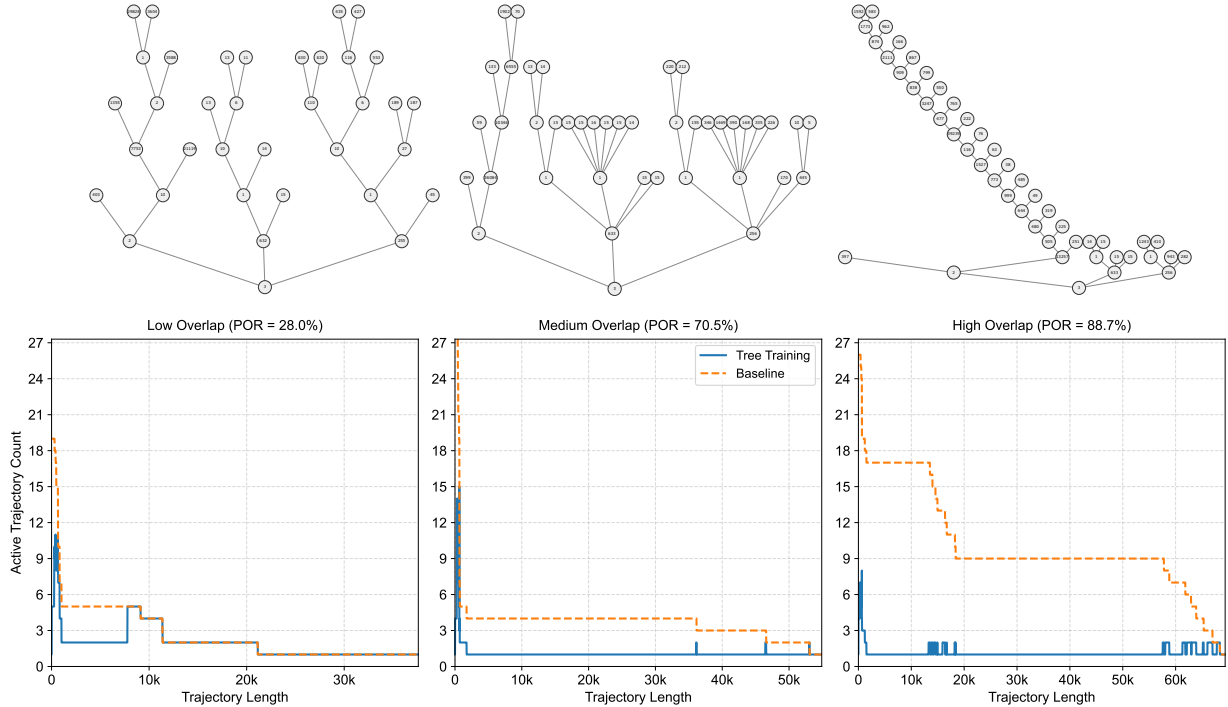


Figure 5. Real agentic trajectory trees and their overlap characteristics. The upper row visualizes representative trajectory trees extracted from multi-turn agentic RL rollouts, exhibiting different degrees of prefix sharing: **Low Overlap**, **Medium Overlap**, and **High Overlap**. The lower row plots the corresponding *active trajectory counts* over trajectory length for both the baseline (dashed) and Tree Training (solid). The area under each curve represents the total number of tokens processed by each method, and the ratio between the baseline and Tree Training areas reflects the theoretical token reuse achievable through tree-based computation sharing.

This demonstrates that the gradient correction also exhibits transitivity within the attention operation, implying that the same correction method used for linear operations can be applied.

Other Operations Taking the Rope operation as a case study, this section explains our general strategy for performing gradient corrections on some specific pointwise operations within the Transformer.

For any pointwise operation $Y_i = f(X_i)$, the gradient with respect to the input, dX , in backpropagation can be calculated as follows:

$$dX_i = dY_i * \frac{\partial Y_i}{\partial X_i} \quad (15)$$

To satisfy the transitivity of gradient correction outlined in Equations 12 and 9, the following condition should be guaranteed:

$$\frac{\partial Y_i^{ours}}{\partial X_i^{ours}} = \frac{\partial Y_i^{base}}{\partial X_i^{base}} \quad (16)$$

For the Rope operation, defined as $Y = \text{Rope}(X, m)$ with

position-dependent m , the gradient $\frac{\partial Y_i}{\partial X_i}$ depends on m . Consequently, it is imperative that the forward pass of Rope in our serialization method uses `position_id` values identical to those in the baseline method. Equation 16 decouples the entire backpropagation chain, allowing us to correct a specific operation without considering the influence of previous or subsequent operators.

3.2.4 Implementation

Building upon the analysis in 3.2.3, our implementation comprises three key components. Firstly, during the forward pass, we implement a **shared prefix attention mask** and correct **position embedding** by aligning each element with its original position in the original trajectory. Secondly, we introduce a **Gradient Scaler** mechanism in the backward pass to compensate for the gradient loss from skipped computations.

Shared Prefix Attention Mask In the forward pass, due to tree packing, we introduce a shared prefix mask to ensure correctness in attention computation. The shared prefix mask is a modified causal mask that restricts the attention scope of each token so that tokens of different trajectories can safely share the same prefix representation without

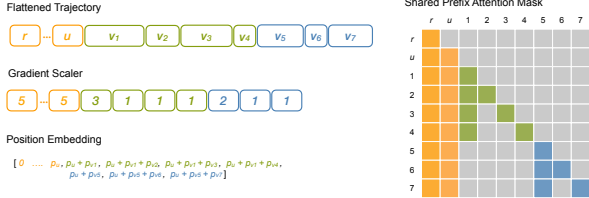


Figure 6. Implementation of flattened tree trajectory. Each flattened tree trajectory requires (1) a gradient scale tensor for prefix reuse, (2) a position embedding tensor that restores original token positions, and (3) a shared-prefix attention mask that enables proper computation reuse across overlapping prefixes during both forward and backward passes.

leaking information across branches. Based on the Flash Attention V3 project (Shah et al., 2024; Wang et al., 2025), we have implemented a high-performance attention GPU kernel with node level shared prefix mask.

Position Embedding The position_ids of the tree-packed data differs from those before packing. Therefore, we need to recompute the position IDs. In sequence packing, position_ids are simply reassigned based on the packed sequence layout. However, in tree training, we must instead restore the original (pre-packing) position IDs onto the packed sequences, so that each token’s positional information remains consistent with its original trajectory. A schematic diagram of the shared prefix mask and position embedding is shown in Figure 6.

Gradient Scaler Based on the analysis in 3.2.3, we can safely recover the correct gradients by scaling. Specifically, after we calculate how many sequences reuse each node in the Tree — a coefficient we call the **tree-scale**, we multiply the gradient of each node by its corresponding tree-scale factor. The workflow of the Gradient Scaler is illustrated in Figure 7.

In the overall training pipeline, we only need to insert a **gradient scaling** step before the backward propagation. This operation restores the correct influence of each sequence’s prefix on the model update, ensuring training consistency. At the same time, for linear-type computations, we can avoid redundant computation on shared prefixes altogether.

Here, the gradient scaler acts as a correction factor that compensates for how many packed sequences share the same prefix. In other words, if a prefix node is reused by multiple sequences, its gradient is scaled accordingly so that the total gradient contribution remains mathematically equivalent to processing each sequence independently.

Parallelism in Distributed System Tree Training is orthogonal to standard parallelism strategies (TP/EP/

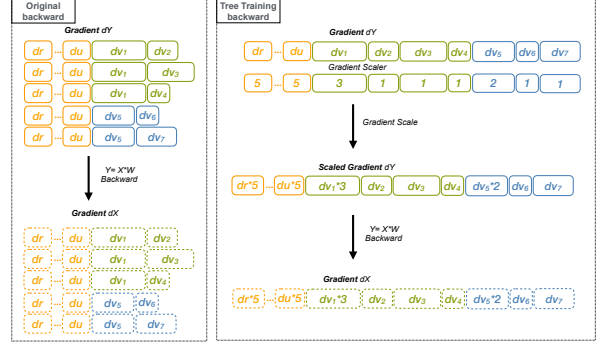


Figure 7. Backward computation with gradient scaling in Tree Training. After the first gradient of the flattened tree trajectory (dY) is computed, the gradient scaler is applied to the gradients of shared prefixes by their reuse counts. For example, the shared prefix $r \rightarrow u$ is used by five trajectories (scale = 5), and v_1 is used by three trajectories (scale = 3), ensuring correct gradient accumulation.

DP/PP) and can be seamlessly combined with them. Context parallelism only affects self attention module. For the self-attention, different ranks receive distinct query shards along with the full key and value tensors per attention head. The attention masks for each parallel rank are generated based on their respective query shards, ensuring the correctness of the implementation.

MoE model load balancing For models without auxiliary loss (e.g., Qwen3 MoE): The tree structure does not affect the load balancing process.

For models with auxiliary loss: We achieve mathematical equivalence to the baseline by multiplying each prefix token by its share count (the gradient scaler) during the router auxiliary loss calculation.

3.3 Tree Packing

In practice, fitting an entire trajectory tree into GPU memory is often infeasible; therefore, we design an efficient packing algorithm that partitions a large computation tree into a sequence of memory-feasible subtrees. The goal is to keep each subtree within a memory limit C while maximizing shared-prefix reuse, thereby minimizing the overall training cost.

Theoretically, the optimal partitioning requires dynamic programming coupled with bin packing, which is NP-hard and computationally prohibitive for large-scale trees due to an exponential state space. Implementation details are provided in the appendix A.

To balance efficiency and performance, we instead adopt a greedy heuristic DFS algorithm that approximates the optimal packing while scaling linearly with tree size. This

approach follows three guiding principles: it prioritizes allocating the deepest leaves first (as they contribute most to the total trajectory length), groups leaves of similar depths within each subtree to improve packing homogeneity, and traverses the tree in depth-first order, initiating a new traversal whenever the accumulated length exceeds capacity C .

To demonstrate the efficiency of this approach, we present a concrete example in Figure 4. Consider a tree-structured dataset containing 4 trajectories with a total of 83k tokens. Assuming a GPU memory limit of $C = 60k$, standard flattening would yield 4 separate sequences totaling 164k tokens due to redundant prefixes. In contrast, our algorithm partitions the tree into two sequences (fitting within C), resulting in a total of only 102k tokens. This significantly reduces both memory usage and computational overhead compared to the baseline.

3.4 Does Tree Training introduce bias in the gradient updates?

Tree Training does not introduce bias during training. This is because our method does not construct trees across different global batch. During training, each global batch is a self-contained tree. The data shuffle operation is applied only between these complete tree samples and never disrupts the internal structure within a tree (as illustrated in the attached "2-illustration-thinking-model-multi-turn.png", where a Global Batch Size (GBS) of 3 corresponds to three independent tree structures).

The fundamental reason is: The set of trajectories forming a single tree does not come from multiple rollouts; instead, the prefix-tree structure is naturally generated from a single rollout. Consequently, the tree packing is organized and processed entirely within one gradient accumulation step. It never involves packing trajectories from different global batches.

4 EXPERIMENTS

We evaluate Tree Training along three dimensions: gradient correctness, efficiency under realistic memory constraints, and end-to-end training performance. Across all settings, reusing shared prefixes from overlapping trajectories substantially reduces redundant computation while preserving equivalence to standard sequence-based baselines.

4.1 Metrics

To clearly separate dataset structure from runtime effects, we define two complementary metrics.

Potential Overlap Ratio (POR) quantifies the theoretical upper bound of computation reuse by measuring the redundancy inherent in shared prefixes. We define POR as the

ratio of overlapping tokens to the total token count of the flattened dataset:

$$\text{POR} = 1 - \frac{N_{\text{tree}}}{N_{X_{\text{base}}(\text{root})}} \quad (17)$$

Here, N_{tree} denotes the token count in the prefix tree, while $N_{X_{\text{base}}(\text{root})}$ represents the token counts of the serialized tree produced by the baseline method described in Equation 3. Using the example from Figure 4, the POR is calculated as $1 - \frac{83k}{164k} \approx 49.4\%$, indicating that nearly half of the baseline computation is redundant.

Effective Reuse Ratio (ERR) evaluates the actual efficiency of computation reuse under memory constraints. It is defined as the fraction of redundant tokens actually eliminated by the optimization:

$$\text{ERR} = 1 - \frac{N_{\text{pack}}}{N_{X_{\text{base}}(\text{root})}} \quad (18)$$

Here, N_{pack} represents the total token count after partitioning the tree. For the scenario in Figure 4, the ERR is calculated as $1 - \frac{102k}{164k} \approx 37.8\%$, demonstrating significant savings despite the memory constraint.

4.2 Evaluation Setups

We evaluate the end-to-end training efficiency by comparing the total time required to process equivalent data between Tree Training and the baseline described in Section 3.2.1. This baseline aligns with the current standard practice for training on branched trajectories, as most existing training frameworks only support taking batch of `list` (tensor) as training inputs.

All experiments were conducted on clusters of 64 NVIDIA Hopper GPUs using Megatron-Core (Shoeybi et al., 2020) for distributed training. Sequence Packing (Krell et al., 2021) is used in our baseline setting, representing the standard batching strategy used in large-scale LLM fine-tuning and RL training.

4.3 Speedup and Correctness on real-world agentic trajectories

To assess real-world applicability, we collect agentic RL rollouts from multi-turn reinforcement learning tasks. Figure 5 presents representative realistic agentic trajectory trees (top) alongside their corresponding token-overlap distributions (bottom). These trajectories are collected from the execution of tasks from agentic scaffold Terminus (`ter`) and Claude code (`cc`). Most branching behaviors of the left two trees are caused by concurrent tool execution and retokenization drift (Luo et al., 2025), while the right tree is caused by the think

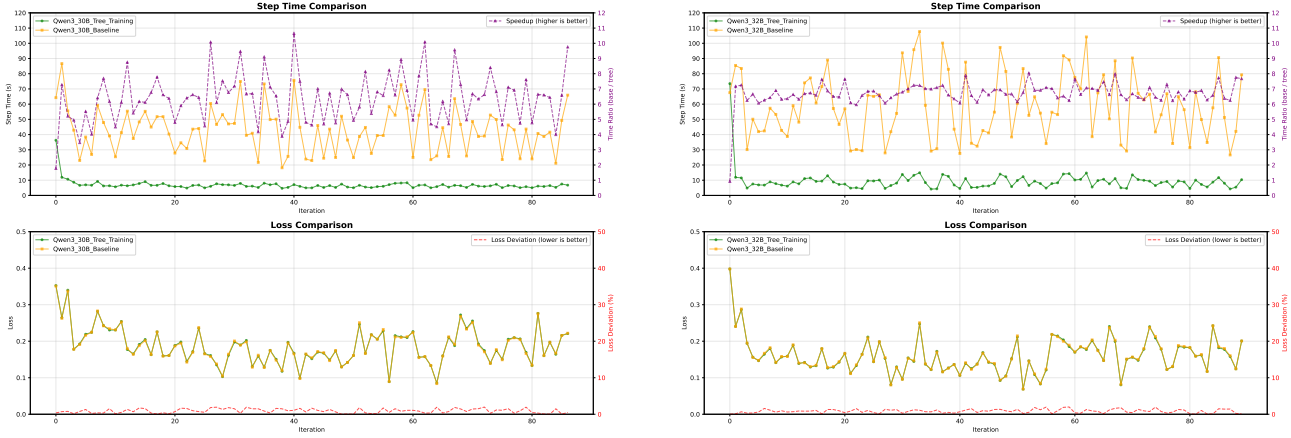


Figure 8. End-to-end training speedup and loss comparison using real world rollout data with think mode turned on. Results for the MoE model Qwen3-30B are shown on the left, and for the dense model Qwen3-32B on the right. For each model, the top plot illustrates the training speedup achieved by Tree Training, while the bottom plot displays the average relative error in loss.

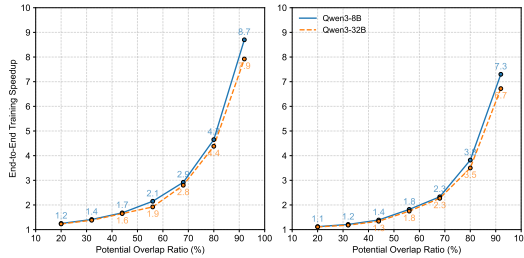


Figure 9. End-to-end training speedup of Tree Training across datasets with varying POR. Each subfigure reports the relative reduction in total training time of Tree Training compared to the baseline. (a) synthetic datasets where the full tree fits in GPU memory, (b) synthetic datasets requiring tree packing under memory constraints.

mode. These examples illustrate a broad spectrum of prefix sharing, ranging from low to high POR (from 28.0% to 88.7%), and reveal that real agentic datasets tend to exhibit sparse, unbalanced trees with highly variable reuse across different depths and branching factors.

To validate the correctness and speedup of our method, we illustrate the loss comparison and step-time comparison on real-world agentic trajectories as shown in Figure 8:

(1) Speedup (Top Panel): The theoretical speedup upper bound $\frac{1}{1-\text{POR}}$ for this dataset is **6.5 \times** . We achieved average realized speedups of **6.3 \times** (32B Dense) and **6.2 \times** (30B MoE). This demonstrates that our system incurs negligible overhead, capturing over **95%** of the theoretical potential. The step-wise fluctuation (2 \times –10 \times) faithfully reflects the varying intrinsic POR of dynamic tree samples.

(2) Correctness (Bottom Panel): Tree Training reproduces the baseline’s loss and gradient behaviors, with numerical deviations consistently maintained within acceptable preci-

sion tolerance. The training loss curves for Baseline (Yellow) and Ours (Green) overlap perfectly. The deviation (Red dashed) is negligible ($\pm 1\%$), confirming strict mathematical equivalence.

4.4 Speedup of datasets with varying POR

For controlled experiments, we construct synthetic datasets with POR values from 20% to 92%, while keeping the number of leaf trajectories and total tokens constant across settings. This setup allows us to systematically study how the overlap degree influences computation reuse and throughput.

As shown in Figure 9, Tree Training consistently reduces total training time across all conditions, with the improvement magnitude increasing monotonically with the Potential Overlap Ratio (POR). In the ideal setting where full trees fit in memory, Tree Training achieves up to 8.7 \times speedup by eliminating redundant computation through shared prefix reuse.

4.5 Memory footprint

In our implementation, even when large trees must be split (achieved via the proposed Tree Packing method), our performance remains close to $\frac{1}{1-\text{ERR}}$, demonstrating that our system incurs negligible runtime overhead.

As shown in table 1, the last column represents the essential minimum storage required for activations with full recomputation. Columns 1, 2, and 3 show the GPU memory footprint for attention masks, original position IDs, and gradient scalars, respectively. s is the sequence length of a packed tree, n is the number of nodes within a single tree ($n \ll s$, for example, a tree is constructed by 40 nodes with a total sequence length of 100k), h stands for hidden states’

Table 1. Memory footprint of additional tensors

	attention masks	original position ids	gradient scalars	baseline
elements count	$n \times n + n$	s	s	$s \times h \times L$
memory cost	$n \times n + n \times 4$	$s \times 4$	$s \times 4$	$s \times h \times L \times 2$
Qwen3-32B	0.0016 MB	0.39 MB	0.39 MB	64000 MB

dimension, and L represents the number of transformer layers. For a 32B model, the additional memory introduced by these components is far smaller than the minimal activation memory footprint.

4.6 The gain of training on all tokens of trajectory trees

Training on all tokens of trajectory trees, compared to training on only a single trajectory (in our baseline experiment, we select the longest trajectory as common practice), leads to a clear performance gain, especially for thinking models.

On Terminal Bench 2.0(Merrill et al., 2026), we use a cold-started Qwen3-32B as the base checkpoint for RL training. The model trained on the full tree (with think-mode turned on) achieves a score (avg@4) of 28.8, whereas the baseline score is 20.9.

5 CONCLUSION

We propose Tree Training, a performance optimization framework during the training phase. It aims to minimize redundant computation and boost efficiency while strictly maintaining the gradient values of the parameters undergoing optimization. In contrast to existing prefix reuse schemes, our Tree Training is not only suitable when the prefix is just a prompt that does not contribute to gradients, but also when the prefix is involved in gradient updates.

REFERENCES

- claude-code. URL <https://claude.com/product/claude-code>.
- Terminus. URL <https://www.tbench.ai/terminus>.
- Abadi, M., Barham, P., Chen, J., Chen, Z., Davis, A., Dean, J., Devin, M., Ghemawat, S., Irving, G., Isard, M., Kudlur, M., Levenberg, J., Monga, R., Moore, S., Murray, D. G., Steiner, B., Tucker, P., Vasudevan, V., Warden, P., Wicke, M., Yu, Y., and Zheng, X. Tensorflow: A system for large-scale machine learning, 2016. URL <https://arxiv.org/abs/1605.08695>.
- Abdelaziz, I., Basu, K., Agarwal, M., Kumaravel, S., Stal-lone, M., Panda, R., Rizk, Y., Bhargav, G. P. S., Crouse, M., Gunasekara, C., Iqbal, S., Joshi, S., Karanam, H., Kumar, V., Munawar, A., Neelam, S., Raghu, D., Sharma, U., Soria, A. M., Sreedhar, D., Venkateswaran, P., Unuvar, M., Cox, D. D., Roukos, S., Lastras, L. A., and Kapanipathi, P. Granite-function calling model: Introducing function calling abilities via multi-task learning of granular tasks. In Dernoncourt, F., PreoŃiu-Pietro, D., and Shimorina, A. (eds.), *Proceedings of the 2024 Conference on Empirical Methods in Natural Language Processing: Industry Track*, pp. 1131–1139, Miami, Florida, US, November 2024. Association for Computational Linguistics. doi: 10.18653/v1/2024.emnlp-industry.85. URL <https://aclanthology.org/2024.emnlp-industry.85/>.
- Cheng, Y., Du, K., Yao, J., and Jiang, J. Do large language models need a content delivery network? *arXiv preprint arXiv:2409.13761*, 2024.
- Cheng, Y., Liu, Y., Yao, J., An, Y., Chen, X., Feng, S., Huang, Y., Shen, S., Du, K., and Jiang, J. Lmcache: An efficient kv cache layer for enterprise-scale llm inference. *arXiv preprint arXiv:2510.09665*, 2025.
- DeepSeek-AI, Liu, A., Feng, B., Wang, B., Wang, B., Liu, B., Zhao, C., Dengr, C., Ruan, C., Dai, D., Guo, D., Yang, D., Chen, D., Ji, D., Li, E., Lin, F., Luo, F., Hao, G., Chen, G., Li, G., Zhang, H., Xu, H., Yang, H., Zhang, H., Ding, H., Xin, H., Gao, H., Li, H., Qu, H., Cai, J. L., Liang, J., Guo, J., Ni, J., Li, J., Chen, J., Yuan, J., Qiu, J., Song, J., Dong, K., Gao, K., Guan, K., Wang, L., Zhang, L., Xu, L., Xia, L., Zhao, L., Zhang, L., Li, M., Wang, M., Zhang, M., Zhang, M., Tang, M., Li, M., Tian, N., Huang, P., Wang, P., Zhang, P., Zhu, Q., Chen, Q., Du, Q., Chen, R. J., Jin, R. L., Ge, R., Pan, R., Xu, R., Chen, R., Li, S. S., Lu, S., Zhou, S., Chen, S., Wu, S., Ye, S., Ma, S., Wang, S., Zhou, S., Yu, S., Zhou, S., Zheng, S., Wang, T., Pei, T., Yuan, T., Sun, T., Xiao, W. L., Zeng, W., An, W., Liu, W., Liang, W., Gao, W., Zhang, W., Li, X. Q., Jin, X., Wang, X., Bi, X., Liu, X., Wang, X., Shen, X., Chen, X., Chen, X., Nie, X., Sun, X., Wang, X., Liu, X., Xie, X., Yu, X., Song, X., Zhou, X., Yang, X., Lu, X., Su, X., Wu, Y., Li, Y. K., Wei, Y. X., Zhu, Y. X., Xu, Y., Huang, Y., Li, Y., Zhao, Y., Sun, Y., Li, Y., Wang, Y., Zheng, Y., Zhang, Y., Xiong, Y., Zhao, Y., He, Y., Tang, Y., Piao, Y., Dong, Y., Tan, Y., Liu, Y., Wang, Y., Guo, Y., Zhu, Y., Wang, Y., Zou, Y., Zha, Y., Ma, Y., Yan, Y., You, Y., Liu, Y., Ren, Z. Z., Ren, Z., Sha, Z., Fu, Z., Huang, Z., Zhang, Z., Xie, Z., Hao, Z., Shao, Z., Wen, Z., Xu, Z., Zhang, Z., Li, Z., Wang, Z., Gu, Z., Li, Z., and Xie, Z. Deepseek-v2: A strong, economical, and efficient mixture-of-experts language model, 2024. URL <https://arxiv.org/abs/2405.04434>.
- Goru, R., Mehta, S., and Jain, P. One-pass to reason: Token duplication and block-sparse mask for efficient fine-tuning on multi-turn reasoning, 2025. URL <https://arxiv.org/abs/2504.18246>.
- Hou, Z., Hu, Z., Li, Y., Lu, R., Tang, J., and Dong, Y. Treerl: Llm reinforcement learning with on-policy tree search, 2025. URL <https://arxiv.org/abs/2506.11902>.
- Ji, Y., Ma, Z., Wang, Y., Chen, G., Chu, X., and Wu, L. Tree search for llm agent reinforcement learning, 2025. URL <https://arxiv.org/abs/2509.21240>.
- Kim, S., Moon, S., Tabrizi, R., Lee, N., Mahoney, M. W., Keutzer, K., and Gholami, A. An llm compiler for parallel function calling, 2024. URL <https://arxiv.org/abs/2312.04511>.
- Krell, M. M., Kosec, M., Perez, S. P., and Fitzgibbon, A. Efficient sequence packing without cross-contamination: Accelerating large language models without impacting performance. *arXiv preprint arXiv:2107.02027*, 2021.
- Kwon, W., Li, Z., Zhuang, S., Sheng, Y., Zheng, L., Yu, C. H., Gonzalez, J. E., Zhang, H., and Stoica, I. Efficient memory management for large language model serving with pagedattention, 2023. URL <https://arxiv.org/abs/2309.06180>.
- Li, Y., Gu, Q., Wen, Z., Li, Z., Xing, T., Guo, S., Zheng, T., Zhou, X., Qu, X., Zhou, W., Zhang, Z., Shen, W., Liu, Q., Lin, C., Yang, J., Zhang, G., and Huang, W. Treepo: Bridging the gap of policy optimization and efficacy and inference efficiency with heuristic tree-based modeling, 2025. URL <https://arxiv.org/abs/2508.17445>.
- Liu, Y., Li, H., Cheng, Y., Ray, S., Huang, Y., Zhang, Q., Du, K., Yao, J., Lu, S., Ananthanarayanan, G., et al. Cachegen: Kv cache compression and streaming for fast large language model serving. In *Proceedings of the ACM SIGCOMM 2024 Conference*, pp. 38–56, 2024.

A TREE PACKING DP SOLUTION

Instead of repeatedly processing shared prefixes, we merge trajectories into a tree structure that explicitly captures shared computation. However, fitting the entire trajectory tree into GPU memory is often infeasible, motivating the need for an efficient partitioning strategy. Tree Packing formulates this as optimizing how to split the computation tree into subtrees under a total trajectory-length budget C , ensuring that each batch stays within capacity while maximizing reuse of shared prefixes to minimize overall training cost.

A.1 Single-Path Packing

Within the trajectory tree, each node represents a token segments shared across multiple rollouts, such as a common prompt or an intermediate environment feedback. Selecting an internal node u and using its root-to- u path as a shared segment allows all descendant leaves to reuse this computation. We first analyze a simplified setting where each training step establishes only a single shared path within the trajectory tree. In this case, a training step selects one node u whose shared and residual trajectory lengths jointly fit within the global capacity C . Dynamic programming is employed to enforce this feasibility constraint and compute the optimal selection efficiently.

Notation and constraint Let $T = (V, E)$ denote the trajectory tree with root r . Each edge $e = (x, y) \in E$ has a length $l(y)$ corresponding to the token length of the child sub-trajectory y . For the root r , $l(r)$ denotes the segment length of the root itself. For nodes $p, q \in V$, define $d(p, q)$ as the total token length along the path from p to q . For an internal node $u \in V$, we define:

- $L(u) = d(r, u)$ is the length of the shared prefix $[r \rightarrow u]$.
- $\mathcal{L}(u)$ is the set of leaves in the subtree rooted at u , and $n_u = |\mathcal{L}(u)|$ its cardinality.
- $R(u) = \sum_{\ell \in \mathcal{L}(u)} d(u, \ell)$ is the total residual length under u .

A node u is *feasible* if it satisfies

$$L(u) + R(u) \leq C. \quad (19)$$

The length saving achieved by selecting u as a shared node is

$$S(u) = (n_u - 1)L(u). \quad (20)$$

If u is infeasible, it cannot be chosen as a shared node in any valid training step.

DP definition with feasibility Define $DP(u)$ as the maximum total length saving achievable while covering the entire subtree rooted at u , using only feasible shared-node selections. If it is impossible to cover all leaves within u 's subtree under the constraint, we set $DP(u) = -\infty$.

The recurrence is:

$$DP(u) = \begin{cases} 0, & \text{if } u \text{ is a leaf,} \\ \max \left\{ \mathbf{1}_{f(u)} \cdot (n_u - 1)L(u), \right. \\ \left. \sum_{v \in \text{child}(u)} DP(v) \right\}, & \text{otherwise.} \end{cases} \quad (21)$$

Here $\mathbf{1}_{f(u)} = 1$ if u is feasible and 0 otherwise. The term $\sum_{v \in \text{child}(u)} DP(v)$ is $-\infty$ if any child v has $DP(v) = -\infty$. Quantities $L(u)$, n_u , and $R(u)$ can be precomputed in a single post-order DFS traversal in $O(|V|)$ time.

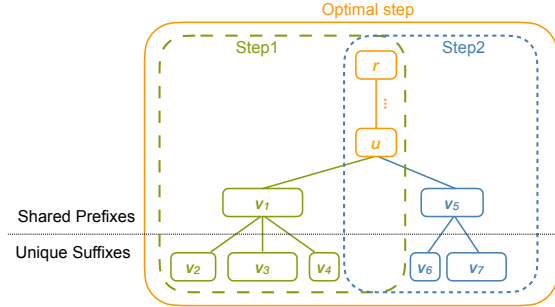


Figure 10. Comparison between single-path and multi-path tree packing. Step 1 packs the shared prefix $r \rightarrow u \rightarrow v_1$, and Step 2 packs $r \rightarrow u \rightarrow v_5$ separately. The optimal strategy instead treats $r \rightarrow u \rightarrow \{v_1, v_5\}$ as a hierarchical shared prefix, enabling greater computation reuse, as discussed in section A.2.

Intuitively, the dynamic program either places a shared prefix at node u , or recursively delegates coverage to its child subtrees. However, restricting each training step to a single shared prefix may fail to achieve maximal reuse, especially when the capacity C is relatively large. As illustrated in Figure 10, packing $r \rightarrow u \rightarrow v_1$ and $r \rightarrow u \rightarrow v_5$ in separate steps leads to redundant computation, whereas the optimal multi-path strategy jointly reuses $r \rightarrow u \rightarrow \{v_1, v_5\}$ as a hierarchical shared prefix. We therefore extend the formulation to the multi-path setting, where multiple shared prefixes can be activated simultaneously within a single training step.

A.2 Multi-Path Tree Packing

We now generalize Tree Packing to the multi-path setting. Selecting an internal node u activates multiple shared paths: the root-to- u path becomes the upper-level shared trajectory, and for each child of u , additional root-to-child trajectories may be nested and reused. In this way, shared

sub-trajectories can branch and overlap, covering multiple subtrees in one step and further reducing the total length, as some sub-trajectories are shared across more leaves.

This leads to a dynamic programming formulation in which each subtree yields a set of candidate states. Parent states are constructed via two operations: (*Lift*) propagating child states upward by adding the edge length, and (*Bin packing*) combining the lifted demands into feasible traversals under capacity C .

Notation We reuse the notation from the single-path setting. The local remaining capacity at node u is

$$C_u = C - L(u). \quad (22)$$

State For each node u , we maintain a candidate set

$$\mathcal{A}_u = \{(\mathbf{b}, \text{cost}(\mathbf{b}))\}, \quad (23)$$

where $\mathbf{b} = (b_1, \dots, b_k)$ is a non-decreasing vector with $0 \leq b_i \leq C_u$. Here, k is the number of traversals that arrive at u , each b_i represents the capacity already used in that traversal upon entering u , and $\text{cost}(\mathbf{b})$ denotes the minimum cumulative length required to cover all leaves in $\mathcal{L}(u)$ under this configuration.

Initialization If u is a leaf, then

$$\mathcal{A}_u = \{((0), 0)\}. \quad (24)$$

Recurrence (child \rightarrow parent) Suppose u has children $\{v_1, \dots, v_m\}$ with corresponding candidate sets \mathcal{A}_{v_j} . We construct \mathcal{A}_u in two steps:

- **Lift:** For each child v and each entry $(\mathbf{t}, \text{cost}_v(\mathbf{t})) \in \mathcal{A}_v$, define

$$\mathbf{t}^{(u)} = \mathbf{t} + w(v) \cdot \mathbf{1}, \quad (25)$$

and keep only those with $\max(\mathbf{t}^{(u)}) \leq C_u$. Each component of $\mathbf{t}^{(u)}$ is treated as an item and inserted into a multiset S , with its associated cost contribution $\text{cost}_v(\mathbf{t})$.

- **Bin packing:** For each feasible packing of S into bins of capacity C_u , let the bin loads be b_1, \dots, b_k (sorted non-decreasingly). This defines the parent state $\mathbf{b} = (b_1, \dots, b_k)$. For each child v , let t_v be the number of bins containing items lifted from v . The total cost is

$$\text{cost}(\mathbf{b}) = \sum_v \text{cost}_v(\mathbf{t}_v) + \sum_v w(v) \cdot t_v. \quad (26)$$

Insert $(\mathbf{b}, \text{cost}(\mathbf{b}))$ into \mathcal{A}_u , keeping only the minimal cost for identical \mathbf{b} .

Termination At the root r , we obtain \mathcal{A}_r . The optimal total length is

$$\text{Cost} = \min_{(\mathbf{b}, c) \in \mathcal{A}_r} c. \quad (27)$$

Complexity and Approximation The multi-path dynamic programming formulation provides a theoretically optimal solution but is computationally expensive in practice. The state space may grow exponentially in the worst case, since each child contributes multiple candidate vectors and their combinations grow multiplicatively across children. Furthermore, the bin-packing step on the multiset S is locally NP-hard.

Thus, the exact DP is tractable only for small to medium trees but remains valuable as a ground truth for evaluating approximations. For larger instances, we complement the exact DP with a heuristic algorithm that approximates the bin-packing step while scaling efficiently to large trees. In practice, the heuristic algorithm follows three guiding principles: it prioritizes allocating the deepest leaves first (as they contribute most to the total trajectory length), groups leaves of similar depths within each subtree to improve packing homogeneity, and traverses the tree in depth-first order, initiating a new traversal whenever the accumulated length exceeds capacity C .